The American Journal of Pathology, Vol. 170, No. 6, June 2007

DOI: 10.2353/ajpath.2007.060898

Molecular Pathogenesis of Genetic and Inherited Diseases

Vacuolar Leukoencephalopathy with Widespread Astrogliosis in Mice Lacking Transcription Factor Nrf2

Ann F. Hubbs,* Stanley A. Benkovic,† Diane B. Miller,† James P. O'Callaghan,‡ Lori Battelli,* Diane Schwegler-Berry,* and Qiang Ma§

From the Experimental Pathology Laboratory, Pathology and Physiology Research Branch, and the Chronic Stress and Neurotoxicology Laboratory,† Molecular Neurotoxicology Laboratory,‡ and Receptor Biology Laboratory,§ Toxicology and Molecular Biology Branch, Health Effects Laboratory Division, National Institute for Occupational Safety and Health, Centers for Disease Control and Prevention, Morgantown, West Virginia*

NFE2-related factor 2 (Nrf2), an oxidant-activated CNC bZip transcription factor, has been implicated in defense against oxidative stress and chemical insults in a range of cell and tissue types, including the central nervous system. Here, we report that deletion of the *Nrf2* gene in mice caused vacuolar (spongiform) leukoencephalopathy with widespread astrogliosis. The leukoencephalopathy was present in all *Nrf2*-null mice more than 10 months of age, was characterized by vacuolar degeneration involving all major brain regions, and was most apparent in the white tracts of the cerebellum and pons. Vacuolar degeneration in white tracts was attributable to myelin unwinding and intramyelinic cysts, and double-label immunofluorescence for 4-hydroxy-2-nonenal and myelin basic protein localized free-radical-induced oxidative damage to the myelin sheath. Moreover, the brains of *Nrf2*-null mice exhibited widespread astrocyte activation with profusion of glial fibrillary acidic protein-immunoreactive glial processes. The study uncovered a possible physiological role for *Nrf2* in maintaining central nervous system myelin. If this role is confirmed, it may suggest new approaches to treating genetically and chemically induced myelin degenerative diseases. ***(Am J Pathol 2007, 170:2068–2076; DOI: 10.2353/ajpath.2007.060898)***

NFE2-related factor 2 (Nrf2), also known as nuclear factor erythroid 2-like 2, is a leucine zipper transcription factor that interacts with the antioxidant response element (Online Mendelian Inheritance of Man no. 600492).[1] Through the regulation of the antioxidant response element, Nrf2 is believed to play a major role in cellular defenses including constitutive expression and induction of phase II xenobiotic metabolizing enzymes as well as protection against oxidant-induced cell injury.[2] In the central nervous system, Nrf2 is hypothesized to prevent oxidant injury in neurons,[3,4] to attenuate NO-dependent neuronal apoptosis,[5] to decrease neuronal injury during cerebral ischemia,[6] and to limit neurodegeneration in models of Huntington's disease. Intracellular levels of Nrf2 are regulated by proteasomal degradation that is controlled by Keap1.[7,8]

We recently reported *Nrf2* deletion induces a lupus-like autoimmune syndrome in female mice characterized by inflammatory lesions in liver and kidney, anti-DNA antibodies, intravascular deposition of IgG, and altered ratios of $CD4^+$ and $CD8^+$ T lymphocytes.[9] Biochemical analysis revealed that mutant mice were lacking certain phase II detoxification enzymes in hepatic and lymphoid cells, rendering the mice unable to maintain peripheral lymphocyte homeostasis and autoimmune surveillance.[9] Brains from these animals were collected and analyzed for the presence of immune-mediated disease and cause of death and morbidity. Although *Nrf2*-null mice did not demonstrate a substantive immune response in brain, and neurological disease did not cause death in these mice, vacuolar (spongiform) leukoencephalopathy was observed in several *Nrf2*-null mice. We were concerned that the absence of Nrf2 was promoting neural damage and/or leukodystrophy, a condition associated with degeneration of myelin, and initiated a systematic evaluation of the brains of *Nrf2*-null mice.

Accepted for publication March 13, 2007.

The findings and conclusions in this report are those of the authors and do not necessarily represent the views of the National Institute for Occupational Safety and Health.

Address reprint requests to Qiang Ma, Receptor Biology Laboratory, Toxicology and Molecular Biology Branch, Health Effects Laboratory Division, National Institute for Occupational Safety and Health, Centers for Disease Control and Prevention, 1095 Willowdale Rd., Morgantown, WV 26505. E-mail: qam1@cdc.gov.

Our standard neurohistological evaluation includes stains that positively depict neuronal damage and glial activation, such as cupric-silver, Fluoro-Jade B, and glial fibrillary acidic protein (GFAP) immunohistochemistry. These stains reveal neuropathological alterations that are not readily observed with standard hematoxylin and eosin (H&E) stains.[10] Fluoro-Jade B is a high-affinity and high-specificity fluorescent stain that facilitates detection of neuronal degeneration.[11,12] In the brain, changes in other cell types can also reflect neuronal injury. In particular, astrocytes respond to neural injury through a hypertrophic process termed "reactive gliosis" that involves increased production of glial intermediate filaments, the major protein component of which is GFAP. Elevation in the GFAP level is a generic biomarker of underlying brain damage and is observed across a variety of central nervous system (CNS) injuries.[10,13–18] To characterize further the morphological changes in the brains of *Nrf2*-null mice, we conducted necropsies using perfusion fixation of control and aged knockout mice before H&E light microscopy and transmission electron microscopy. Finally, we performed immunohistochemical staining to identify Iba-1, a calcium-binding protein that reveals microglial activation state, and to localize sites of oxidant injury using immunofluorescent double labeling for the lipid peroxidation product 4-hydroxy-2-nonenal and the myelin marker myelin basic protein. These morphological and neurohistochemical studies revealed the presence of a unique vacuolar leukoencephalopathy with myelin unwinding, intramyelinic cysts, and widespread astrogliosis in mice lacking Nrf2.

Materials and Methods

Mice

Nrf2 knockout mice with a 129/SvJ background were generously provided by Dr. Y.W. Kan (University of California, San Francisco, CA)[19] and were re-derived at The Jackson Laboratory (Bar Harbor, ME) to ensure that the mice were free of specific pathogens. *Nrf2* knockout and wild-type 129/SvJ mice were housed in the environmentally controlled National Institute for Occupational Safety and Health barrier facility, which is fully accredited by the Association for Assessment and Accreditation of Laboratory Animal Care International. The mice were provided with water and an irradiated diet (Harlan Teklad 7913; Harlan Teklad, Madison, WI) *ad libitum*. They were housed in microisolator cages on sterile Beta chip bedding (Northeastern Products, Warrensburg, NY) and received positive pressure HEPA-filtered air to each individual cage using a Maxi-Miser System (Thoren Caging Systems, Hazleton, PA).

For neuropathology analysis, *Nrf2*-null mice ages 1 year or older without clinical renal failure were used for necropsy. The *Nrf2*-null mice had a mean (±SE) age of 15.7 ± 1.5 months and a median age of 14 months (range, 12 to 25 months); six were female and five male. Control wild-type 129/SvJ mice had a mean (±SE) age of 12.3 ± 1.3 months and a median age of 14 months (range from 6 to 14 months); three were female and three male. Only one of the wild-type mice was less than 1 year of age.

For brain GFAP and Fluoro-Jade B staining, male *Nrf2*-null mice over 10 months of age without clinical renal failure were selected for necropsy. Three wild-type 129/SvJ and two wild-type C57BL/6J mice over 9 months of age were used as controls. For Iba-1 staining and for the immunofluorescence studies, an additional four *Nrf2*-null and four wild-type male mice over 15 months of age were used.

Neuropathology Necropsies

Surveillance necropsies were conducted as previously described.[9] Mice were observed for signs of illness daily. Mouse breeding, morbidity, and mortality were recorded using the Colony software, version 3.0 (Locus Technology, Inc., Orland, ME). Brain tissues from surveillance necropsies were preserved by immersion in 10% neutral buffered formalin.

For systematic neuropathology examinations, brains were preserved for neuropathology as previously described.[20] In brief, mice were deeply anesthetized by intraperitoneal injection of pentobarbital (Sleepaway; Fort Dodge Laboratories, Fort Dodge, IA), intravascularly perfused via the heart with 25 ml of calcium- and magnesium-free phosphate-buffered saline (PBS) containing heparin (10 units/ml) at 100 cc of pressure, followed by intravascular perfusion with room temperature Karnovsky's fixative.[21] For light microscopy, three cross sections of brain from 11 *Nrf2*-null and six control mice were collected as previously described[22] and embedded in paraffin. For electron microscopy, specimens of the left cerebellar white tracts, pontine white tracts, and cerebellar vermis from six of the *Nrf2*-null and four of the control mice were postfixed in 1% osmium tetroxide and embedded in Epon. Ultrathin sections were cut at 70 nm, collected onto copper grids, and stained with uranyl acetate and lead citrate. Ultrastructural sections were viewed and photographed using a JEOL JEM-1220 analytical transmission electron microscope (Tokyo, Japan).

For histopathology evaluation, morphological alterations in the brains of *Nrf2*-null and wild-type mice were evaluated by a board-certified veterinary pathologist (A.F.H.). Light microscopic changes in H&E-stained sections were separately scored for severity and distribution on a scale of 0 to 5, and the two scores were added to produce a semiquantitative pathology score as previously described.[23]

Five *Nrf2*-null mice and five wild-type mice were used for GFAP immunohistochemistry and Fluoro-Jade B staining. An additional four null and four wild-type mice were used for Iba-1 immunohistochemistry and double-labeled immunofluorescent staining to simultaneously detect myelin basic protein and the lipid peroxidation product 4-hydroxy-2-nonenal. Mice were deeply anesthetized with pentobarbital (Sleepaway) and perfused transcardially with 100 ml of 0.9% saline followed by 150 ml of 4% paraformaldehyde. Brains were removed from the skulls

and postfixed overnight in the perfusion solution. Following a rinse in Dulbecco's phosphate-buffered saline (DPBS), brains were cryoprotected for 24 hours each in 10, 20, and 30% sucrose in DPBS. Frozen sections were cut at 35 microns on a Leica cryostat (model CM3000) and collected in DPBS + 0.8 g/L sodium azide.

Immunoperoxidase Staining

To visualize GFAP (astrocytic) and Iba-1 (microglial) immunoreactivity, free-floating sections were stained using the ABC method. Sections were rinsed in DPBS three times for 5 minutes each. Endogenous peroxidase activity was blocked by incubation in 3% H_2O_2 + 10% methanol in DPBS for 15 minutes. Following three more rinses, sections were permeabilized (1.8 g of poly-L-lysine, 20 ml of 5% Triton X-100, 4 ml of equine serum, and 76 ml of DPBS) for 30 minutes, and incubated with GFAP (1:10,000 dilution, 4% equine serum; DAKO, Carpinteria, CA) or Iba-1 antisera (1:250 dilution, 4% equine serum; Wako, Richmond, VA) overnight at 4°C. The next day, sections were brought to room temperature, rinsed three times with DPBS, and incubated with species-appropriate secondary antisera [1:10,000 (GFAP), 1:1000 (Iba-1), 4% equine serum; Vector Laboratories, Burlingame, CA] for 2 hours at room temperature. Following three rinses with DPBS, sections were incubated with Avidin-D horseradish peroxidase (1:1000; Vector Laboratories, Burlington, CA) for 1 hour at room temperature. Sections were rinsed three times and incubated with a Chromagen solution [25 mg/50 ml of 3-3′ diaminobenzidine (Sigma, St. Louis, MO) in DPBS + 50 μl of 30% H_2O_2] for 5 minutes. Following three rinses, sections were mounted onto microscope slides (Colorfrost Plus; Fisher Scientific, Pittsburgh, PA), dehydrated through an ethanol series, and coverslipped with Permount (Fisher Scientific).

Stained sections were viewed with an Olympus BX-50 microscope (Lake Success, NY) equipped with a Spot II digital camera (Diagnostic Images, Sterling Heights, MI) controlled by a Macintosh G4 computer (Apple Computer, Inc., Cupertino, CA). Images were captured with Spot 4.5 software and were assembled and labeled in Photoshop CS2 (Adobe Systems, Mountain View, CA) following image resizing only.

Fluoro-Jade B Staining

Selected sections were stained with Fluoro-Jade B, a fluorescent marker for the localization of degenerating neurons, which was obtained as a gift from Dr. Larry Schmued (National Center for Toxicological Research/Food and Drug Administration, Jefferson, AR).[11] Unstained sections were mounted onto microscope slides (Colorfrost Plus) and were immersed in a solution of 1% NaOH in 80% ethanol for 5 minutes, followed by 70% ethanol for 2 minutes, and distilled water for 2 minutes. Background staining was suppressed by incubation in 0.06% potassium permanganate for 10 minutes with shaking. A rinse in distilled water for 2 minutes was followed by immersion in the staining solution for 20 minutes (0.01% stock solution, 4 ml of stock solution diluted in 96 ml of 0.1% acetic acid). After staining, slides were washed three times in distilled water for 1 minute each and were allowed to air dry overnight. Slides were placed on a warmer at 55°C for 5 minutes, cleared in xylene for 5 minutes, and coverslipped with DPX (Fluka, Buchs, Switzerland).

Immunofluorescent Double Labeling for Myelin Basic Protein and 4-Hydroxy-2-Nonenal

4-Hydroxy-2-nonenal is a common lipid peroxidation product resulting from oxidative stress. Because response to oxidative stress is controlled by Nrf2, we hypothesized that myelin degeneration in *Nrf2*-null mice could result from oxidant injury within the myelin sheath. Therefore, we used immunofluorescence to co-localize 4-hydroxynonenal and myelin basic protein.

Brain sections were mounted on Probe-On Plus slides (Fisher Scientific) and allowed to adhere for 1 day at room temperature. Slides were rehydrated in PBS for 5 minutes, blocked with 5% bovine serum albumin in PBS for 5 minutes, rinsed with PBS, and then blocked with 5% porcine serum (Biomeda, Foster City, CA) for 10 minutes at room temperature in a humidity chamber. Excess liquid was blotted away, and the slides were incubated overnight at 4°C in a humidity chamber with a 1:40 dilution of goat anti-human myelin basic protein (Santa Cruz Biotechnology, Santa Cruz, CA) and rabbit anti-4-hydroxy-2-nonenal (AlphaDiagnostic, San Antonio, TX). The slides were rinsed three times in PBS and incubated for 2 hours at room temperature with a 1:40 dilution in PBS of Alexa Fluor 488 donkey anti-rabbit and Alexa Fluor 594 donkey anti-goat IgG (Molecular Probes/Invitrogen, Carlsbad, CA). For the negative control, rabbit serum (Biogenex, San Ramon, CA) was substituted for primary antibody.

Visualization of Immunofluorescent Double Labeling

Slides were visualized with an Olympus AX-70 photomicroscope equipped with a Quantix Digital camera (Photometrics, Tucson, AZ) and QED camera software (QED Imaging, Inc., Pittsburgh, PA). Fluorescence images were captured in monochrome using green (460 to 500 nm excitation) and red (532.5 to 587.5 nm excitation) cubes. The QED software adds green and red pseudocolor back into these monochrome images to reproduce the fluorescent colors of these cubes with images displayed as single-labeled as well as double-labeled images.

Results

Spontaneous Leukoencephalopathy in Nrf2-Null Mice

Mice with targeted disruption of the *Nrf2* gene exhibited certain disease manifestations and mortality. Both clinical

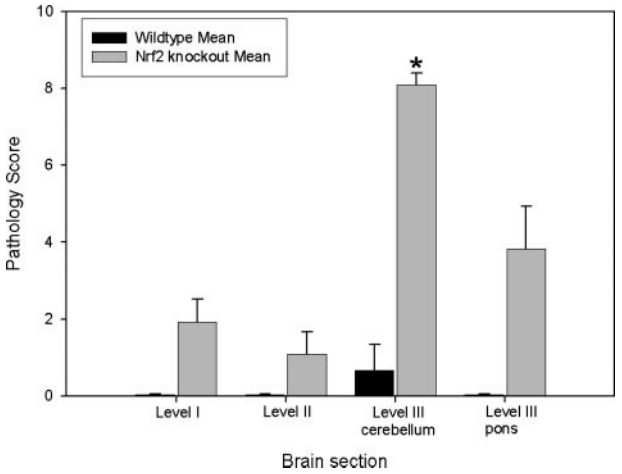

Figure 1. Distribution of vacuolar degeneration in three standard transverse microscopic sections of mouse brain. $^{*}P = 0.001$; Mann-Whitney rank sum test.

and pathological examinations revealed that a majority of the diseased mice developed a lupus-like autoimmune syndrome characterized by multiorgan inflammatory lesions, intravascular deposition of immunoglobulin complexes, and premature death due to rapidly progressing membranoproliferative glomerular nephritis with a female predominance.[9] A diagnostic examination of the brain specimens of the mice using standard light microscopy, formalin-fixed tissue, and H&E-stained sections, in which at least one section of the brain was examined, revealed marked vacuolar leukoencephalopathy characterized by formation of vacuoles in the white matter of the brain (see below). The prevalence of vacuolar leukoencephalopathy was 54% (7 of 13 mice). No apparent gender bias was observed for the brain lesion. The mean age of the mice with vacuolar leukoencephalopathy was 8.3 ± 2.6 months (mean ± SE), whereas the mean age of the mice without evidence of vacuolar leukoencephalopathy was 5.2 ± 1.7 months (mean ± SE). This prevalence rate of 54% in the diagnostic series represents a minimal prevalence rate for vacuolar leukoencephalopathy in the mice examined because of the use of formalin fixation and the absence of level III sections for some mice. Thus, a systematic evaluation of the brain for spontaneous neurodegenerative lesions associated with the absence of the Nrf2 transcription factor was performed.

To systematically evaluate leukoencephalopathy in *Nrf2*-null mice and to distinguish it from other lesions described previously,[9] clinically healthy *Nrf2*-null mice of both genders were chosen for neuropathological evaluation at three standard brain sections.[22] *Nrf2*-null mice at ~1 year and older were found to have vacuolar leukoencephalopathy with a prevalence of 100% (11 of 11). All levels of the brain showed vacuolar leukoencephalopathy, but the pathology scores reached statistical significance only in the cerebellar white tracts ($P = 0.001$, Mann-Whitney rank sum test, Figure 1), where the prevalence was 100%. In level III pons (Figure 2), 6 of 11 *Nrf2*-null mice had multifocal to multifocal and coalescent, moderate to marked, vacuolar degeneration of the pontine white tracts. Light microscopic examination of H&E-stained sections revealed foci of vacuolar degeneration in six and three of the *Nrf2*-null mice in levels I and II, respectively. In the age- and gender-matched wild-type mice in this series, only one animal had a locally extensive area of mild vacuolar degenerative changes in the cerebellar white tracts. There were no other lesions in the brains of wild-type mice.

Microscopically, subgross examination of the brain revealed rarefaction within the cerebellar and pontine white tracts (Figure 2A). At higher magnifications, these foci of rarefaction represented vacuolar (spongiform) degeneration of the cerebellar and pontine white tracts (Figure 2B). The morphological alterations were characterized by multifocal and coalescing cyst-like spaces (Figure 2C) that replaced much of the white matter normally seen in the cerebellum of the wild-type mice (Figure 2D). Foci of vacuolar degeneration in levels I and II were morphologically similar, although less extensive and less consistently observed than in level III. Neither gross examination of the brains nor gross measurements of the different brain levels detected any evidence of cerebellar atrophy.

In the *Nrf2*-null mice, multiloculated cystic dilation of myelin was a consistent ultrastructural finding (Figure 3). The lesion was observed in the pontine white tracts of all *Nrf2*-null mice examined, in the left cerebellar white tracts of three of the five *Nrf2*-null mice, and in the white tracts of the cerebellar vermis of one mouse. Typical lesions included large multiloculated cystic spaces and whorls of myelin within the myelin sheaths of axons (Figure 4A). Severe vacuolar degeneration with associated fibrous astrocytes was seen in the cerebellar vermis of an *Nrf2*-null mouse (Figure 4B). Oligodendrocytes, the cells that secrete and maintain myelin in the central nervous system, were morphologically normal even when adjacent to cystic spaces. Rare aggregates of glial cells were observed (Figure 3B). In the wild-type mice, ultrastructural alterations in the cerebellar vermis, left cerebellar white tracts, and pontine white tracts were limited to low levels of vacuolation within the neuropil, between axons (glial cell vacuolation) in the cerebellar vermis of one mouse, and low levels of myelin splitting in three of the four mice. These were considered to be within the normal limits of the mice (Figure 3A). Together, the results revealed that loss of Nrf2 function caused vacuolar leukoencephalopathy in multiple white tracts of mouse brain that is primarily manifested as cystic dilation of myelin sheaths in the absence of apparent exposure to toxicants, thus implicating Nrf2 in the physiological maintenance of myelin integrity and function. Likewise, the lack of Nrf2 function is related to the pathogenesis of spongiform myelin degeneration in the knockout model.

Widespread Astrogliosis in Nrf2-Null Mice in the Absence of Neurodegeneration

The high prevalence of vacuolar leukoencephalopathy, which primarily affects the myelin sheath, prompted us to examine whether the loss of *Nrf2* caused damage to neurons. Fluoro-Jade B, a specific stain for neuronal damage,[11,12] revealed no significant neuronal degener-

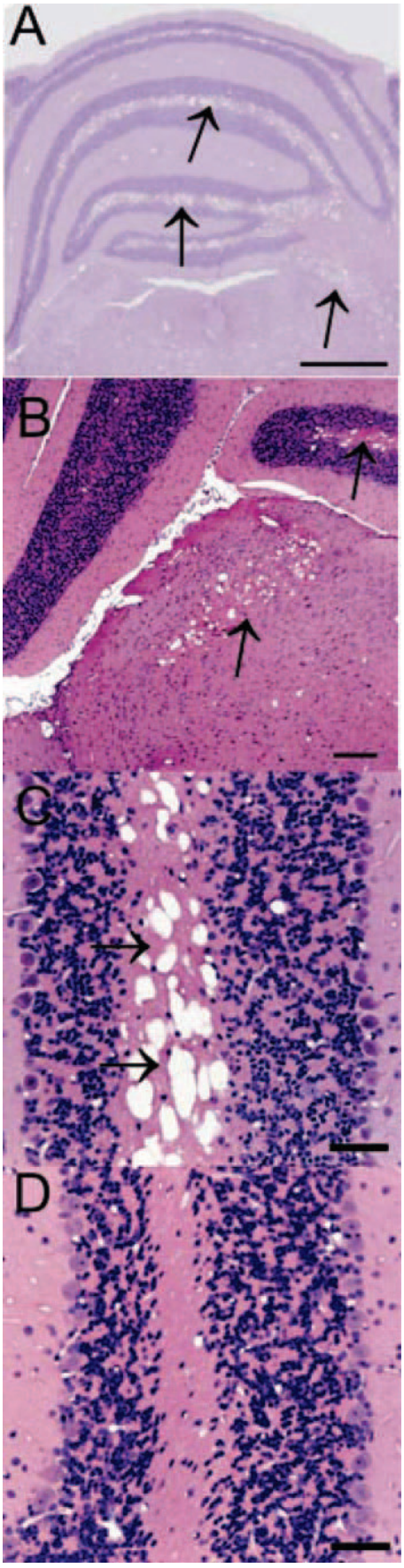

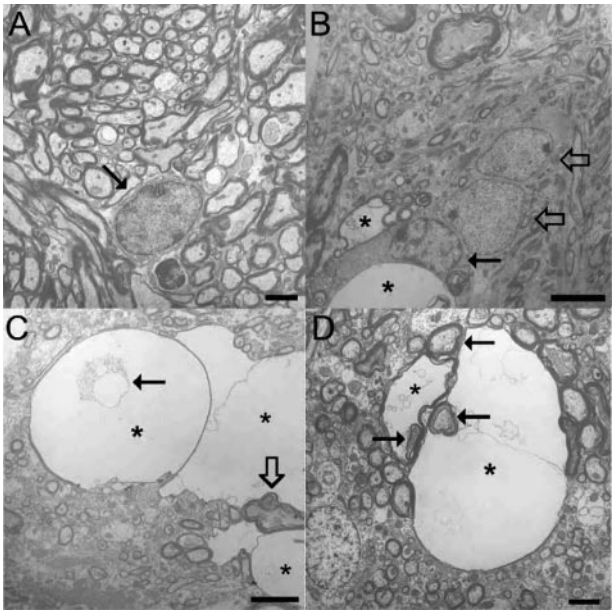

Figure 3. Transmission electron microscope photomicrographs from pontine white tracts. **A:** Pontine white tract from age- and gender-matched wild-type mice. A healthy oligodendrocyte (**arrow**) is amid normally myelinated fibers. Bar = 2 μm. **B:** Pontine white tract from an *Nrf2*-null mouse. Two glial cells consistent with astrocytes (**open arrows**) are adjacent to a morphologically normal oligodendrocyte (**solid arrow**). However, myelin unwinding and intramyelinic spaces (*) are adjacent to this oligodendrocyte. Bar = 5 μm. **C:** Intramyelinic cystic spaces (*) in *Nrf2*-null mice sometimes contain structures consistent with degenerating axons (**solid arrow**), whereas other cysts (*) surround more morphologically normal axon lined by splitting and whirling myelin (**open arrow**). Bar = 1 μm. **D:** Many intramyelinic cystic spaces (*) in the pontine white tracts have clear association with myelinated axons (**arrows**). Bar = 2 μm.

ation or death in the brains of *Nrf2*-null or wild-type mice (Figure 5), despite the striking vacuolation in the white tracts. Immunostaining for Iba-1, a calcium-binding protein that reveals microglial activation state, showed no differences in distribution or morphology of microglia between *Nrf2*-null or wild-type mice, indicating microglial activation is not enhanced by myelinopathy observed in *Nrf2-null mice (data not shown).*

The astrocyte, a major glial cell type in the CNS, can be activated in response to a wide range of neuronal insults, and increased production of the intermediate filament GFAP is a hallmark of astroglial activation and reactive gliosis.[13–15,24] Deletion of the *Nrf2* gene was associated with the activation of astrocytes throughout all major brain regions, especially evident in white matter, and resulted in elevated GFAP immunoreactivity and characteristic astrocytic hypertrophy. Low-magnification microscopy revealed the magnitude of astroglial activation caused by *Nrf2* deletion (Figure 6, B, D, and F) compared with wild-type controls (Figure 6, A, C, and E). In striatum,

Figure 2. Characteristic neuropathological findings in H&E sections. **A:** Photomicrograph of the cerebellum and pons of *Nrf2*-null mice. Spongiform degeneration in the cerebellar and pontine white tracts (**arrows**) caused the degenerating tissue to be paler than adjacent, more normal white matter. Bar = 1 mm. **B:** A higher magnification of vacuolar degeneration in cerebellar and pontine white tracts. Bar = 200 μm. **C:** A higher magnification of the cerebellum from an *Nrf2*-null mouse showing multiple spaces within the white matter. Bar = 50 μm. **D:** Cerebellum from a control mouse. Bar = 50 μm.

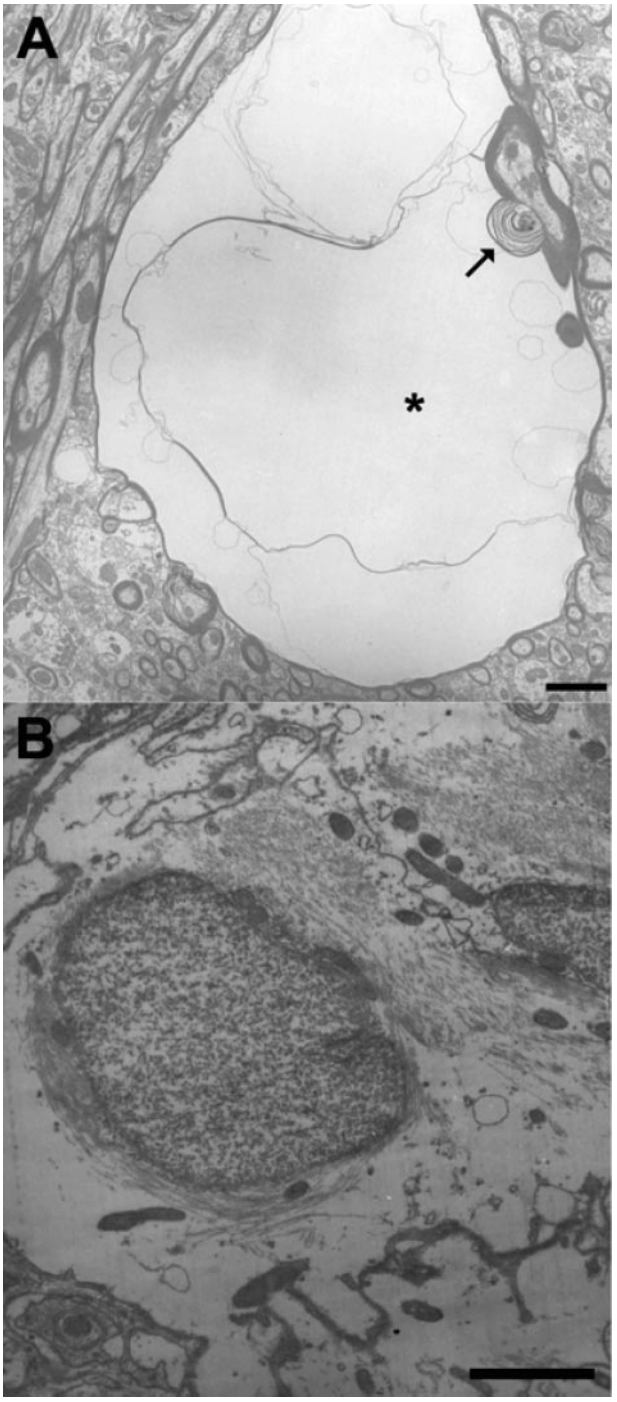

Figure 4. Two types of vacuolar changes in the white tracts of *Nrf2*-null mice. **A:** Vacuolar degeneration in *Nrf2*-null mice was usually characterized by large multiloculated cystic spaces (*) and whorls of myelin within the myelin sheaths of axons (**arrow**). Bar = 2 μm. **B:** A fibrous astrocyte within a focus of vacuolar change in the cerebellar vermis of an *Nrf2*-null mouse. A large amount of fibrillar material was shown in the paranuclear area. Bar = 2 μm.

immunoreactive astrocytes were observed throughout the striatal neuropil of *Nrf2*-null mice (Figure 6B) and were virtually absent from control animals (Figure 6A). The corpus callosum was heavily laden with hypertrophic astroglia (Figure 6B) compared with the wild-type control (Figure 6A). In the hippocampus of *Nrf2*-null animals,

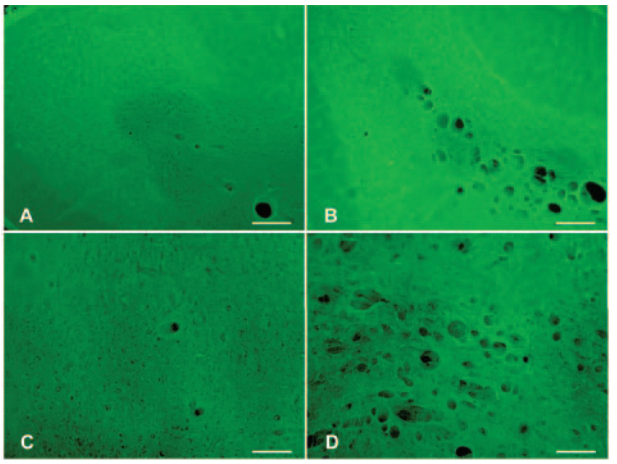

Figure 5. Fluoro-Jade B staining reveals no neurodegenerative changes in *Nrf2*-null mice. Fluoro-Jade B staining revealed no obvious neuronal damage in the cerebellum or pons of *Nrf2*-null mice (**B**, **D**) compared with wild-type control (**A**, **C**). However, the background fluorescent staining revealed *Nrf2* deletion was associated with a severe disruption of white matter tracts throughout the brain and the pontine parenchyma (**B**, **D**). Bar = 100 μm.

elevated immunoreactivity was observed throughout the neuropil and within the hilus (Figure 6D). Especially evident was the immunoreactivity of astrocytes in alveus and tapetum (Figure 6D), which was virtually absent from the

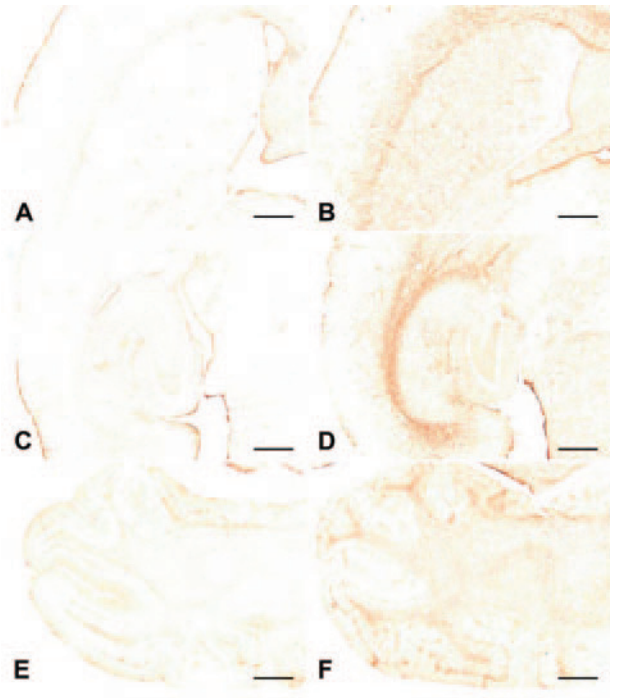

Figure 6. Nrf2 deletion caused reactive gliosis. Targeted deletion of the *Nrf2* gene resulted in the activation of astrocytes throughout the brain but especially evident in white matter tracts. In wild-type control mice, GFAP immunoreactivity was virtually absent in striatum (**A**); however, the *Nrf2*-null mice displayed an intense gliosis throughout the striatal neuropil and the surrounding corpus callosum (**B**). In hippocampus, wild-type animals showed minimal basal immunoreactivity for GFAP (**C**). The *Nrf2*-null mice had increased immunoreactivity in hippocampal neuropil and within the hilus of the dentate gyrus and severe gliosis in the surrounding white matter of the alveus and tapetum (**D**). GFAP immunoreactivity was minimal in the wild-type cerebellum (**E**) but was greatly enhanced throughout the cerebellar white matter by deletion of *Nrf2* (**F**). Bar = 500 μm.

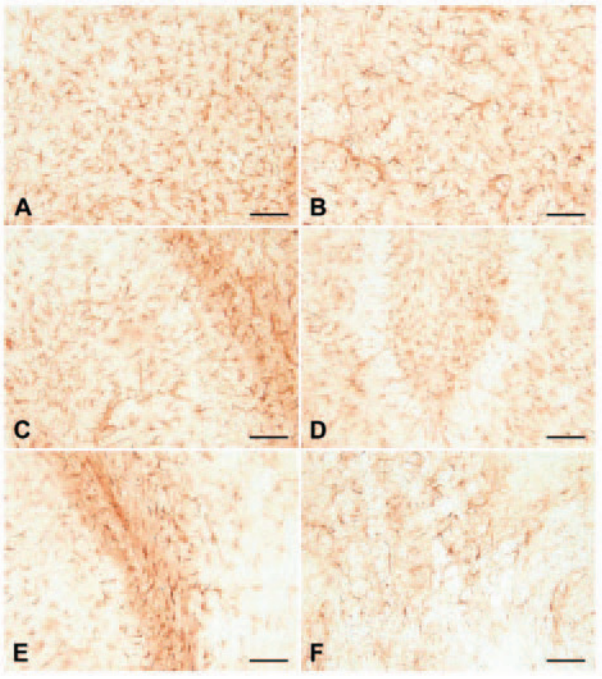

Figure 7. Magnitude of reactive gliosis in major brain regions. Brains from mice containing a targeted deletion of the *Nrf2* gene display brainwide astrocytic hypertrophy. Elevated immunoreactivity for GFAP was observed in astrocytes in the corpus callosum (**A**), throughout the striatum (**B**), within all lamina of the hippocampus (**C**), in the molecular layers and hilus of the dentate gyrus (**D**), in the hippocampal alveus and tapetum (**E**), and throughout the white matter of the cerebellum (**F**). Bar = 200 μm.

controls (Figure 6C). The cerebellum of *Nrf2*-null mice contained many activated astrocytes dispersed throughout all white matter tracts (Figure 6F) compared with wild-type control animals (Figure 6E).

Consistent with widespread astrocyte activation, GFAP immunoreactivity was elevated in all major brain regions of *Nrf2*-null mice (Figure 7). Activated astrocytes were observed throughout the radiato corporis callosi (Figure 7A), dispersed throughout the entire striatal neuropil (Figure 7B), in all hippocampal subregions (Figure 7C), within the hilus and throughout the molecular layers of the dentate gyrus (Figure 7D), within the hippocampal alveus and tapetum (Figure 7E), and throughout the cerebellar white matter (Figure 7F). The coexisting myelin degeneration and astrocyte activation suggests an astrocytic response to myelinopathy and/or dysregulation of the *GFAP* gene associated with *Nrf2* deletion.

4-Hydroxy-2-Nonenal Is Coexpressed with Myelin Basic Protein

The lipid peroxidation product 4-hydroxy-2-nonenal was frequently expressed in white tracts of *Nrf2*-null mice where it co-localized with myelin basic protein to the sites of vacuolar degeneration (Figure 8, A–C). This indicated peroxidation of the lipid component of the myelin sheath. In *Nrf2*-null mice, and to a lesser extent in wild-type mice, 4-hydroxy-2-nonenal was occasionally expressed in the cytoplasm of cells that did not express myelin basic protein.

Discussion

Deletion of Nrf2, an antioxidant-activated transcription factor important in the defense of oxidative and chemical stresses, has uncovered an important function of Nrf2 in the maintenance of myelin homeostasis. Specifically, mice deficient in Nrf2 develop spongiform leukoencephalopathy characterized by degeneration of myelin in the white tracts of the brain without apparent neuronal damage. Myelin degeneration was accompanied by widespread reactive gliosis as assessed by GFAP immunohistochemistry.

Myelin, the insulating layers of membrane wrapped around axons by oligodendrocytes, is essential for normal impulse conduction in the CNS.[25] Aberrant structure and function of myelin can result from defects in the formation of myelin, or myelin degeneration, and result in various CNS disorders including death.[25,26] The leukoencephalopathy and astrogliosis observed in *Nrf2*-null mice appears consistent with a new leukodystrophy because it is a condition characterized by progressive destruction of myelin due to a metabolic defect. Morphologically, the

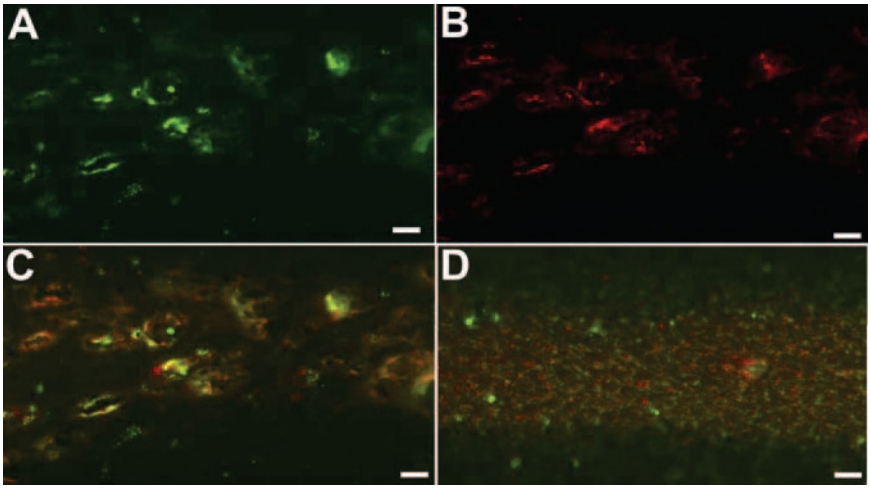

Figure 8. The myelin sheath of *Nrf2*-null mice, but not wild-type mice, demonstrates oxidant injury as reflected in accumulation of 4-hydroxy-2-nonenal (HNE) localized within the myelin sheath by immunofluorescent double labeling for HNE and myelin basic protein (MBP). **A:** HNE, demonstrated by indirect immunofluorescence labeling with rabbit anti-HNE and Alexa Fluor 488 donkey anti-rabbit IgG, appears green and appears to be localized within the dilated myelin sheaths in the cerebellar white tract of a *Nrf2*-null mouse. **B:** MBP, demonstrated by indirect immunofluorescence labeling with goat anti-MBP and Alexa Fluor 594 donkey anti-goat IgG, appears red and labels dilated myelin sheaths in the cerebellar white tract of a *Nrf2*-null mice. **C:** When viewed underneath both red and green fluorescence, HNE co-localizes to sites of MBP expression in *Nrf2*-null mice. **D:** Only low-level HNE (green) fluorescence on nondilated myelin sheaths containing MBP (red) is seen in the double label in the cerebellar white tract of a wild-type mouse. Bar = 20 μm.

leukoencephalopathy of *Nrf2*-null mice is similar to leukoencephalopathy with vanishing white matter in humans, a disease caused by mutations in the subunits of the translation initiation factors, and is characterized by rarefaction and cystic vacuolar degeneration of white matter.[27,28] However, leukoencephalopathy with vanishing white matter generally involves hypomyelination and oligodendrocyte abnormalities suggesting dysmyelination. Based on the cystic vacuolation of myelin and normal oligodendrocytes observed in the *Nrf2*-null mice, and the survival of the mice into adult life, the vacuolar leukoencephalopathy consistently associated with the absence of Nrf2 seems, instead, to be a result of myelin degeneration. The neuropathologic changes in *Nrf2*-null mice also have similarities to the gliosis and intramyelinic vacuolation noted in mice lacking mitochondrial superoxide dismutase[29,30]; however, in the latter case, vacuolation was also observed in the cortex and in brainstem nuclei, areas that were relatively spared in *Nrf2*-null mice. Thus, the unique pathological features of the leukoencephalopathy of *Nrf2*-null mice and the notion that Nrf2 is essential for up-regulation of antioxidant responses to oxidant injury suggest that the intramyelinic vacuolar leukoencephalopathy may represent a new type of leukodystrophy that is caused by impaired myelin homeostasis due to oxidative myelin damage and degeneration in the absence of Nrf2 activation of antioxidant responses.

Although neurodegeneration as assessed by Fluoro-Jade B staining was not evident throughout brain regions of the *Nrf2*-null mice, the widespread astrogliosis was a prominent feature and was especially evident in the white tracts where vacuolar degeneration was also apparent. Such a coexistence of astrogliosis and myelin degeneration has been observed in other natural and experimental disorders/diseases of CNS myelin,[31–33] suggesting myelin degeneration can activate astrocytes. Indeed, demyelination has been shown to be a major stimulus for the subsequent induction of astrogliosis.[14] Our analysis of microglial activation status revealed no apparent differences between wild-type and knockout mice; however, the wild-type animals were a median age of 18 months old and may have some age-related basal microglial activation, or the microglia may have been previously activated and returned to a ramified state while the astrocyte activation was persistent. Future studies will be required to fully determine the extent of age-dependent microglial activation and free radical-induced lipid peroxidation of myelin.

It is reasonable to hypothesize that myelin degeneration in *Nrf2*-null mice could result from oxidant injury within the myelin sheath in the absence of antioxidant responses. The localization of the lipid peroxidation product 4-hydroxy-2-nonenal to the dilated myelin of *Nrf2*-null mice is consistent with this hypothesis. Our findings demonstrate the importance of Nrf2 to normal myelin homeostasis and suggest that in its absence, oxidant injury leads to degeneration of the myelin sheath. Thus, the *Nrf2*-null mouse has a vacuolar leukoencephalopathy, which is a new member of the leukodystrophies, and seems to be associated with oxidant injury that accumulates within the myelin sheath in the absence of Nrf2.

Acknowledgment

We gratefully acknowledge the helpful suggestions of Robert H. Garman, CVM, DACVP.

References

1. Chan K, Han XD, Kan YW: An important function of Nrf2 in combating oxidative stress: detoxification of acetaminophen. Proc Natl Acad Sci USA 2001, 98:4611–4616
2. Kwong M, Kan YW, Chan JY: The CNC basic leucine zipper factor, Nrf1, is essential for cell survival in response to oxidative stress-inducing agents. Role for Nrf1 in gamma-gcs(l) and gss expression in mouse fibroblasts. J Biol Chem 1999, 274:37491–37498
3. Shih AY, Johnson DA, Wong G, Kraft AD, Jiang L, Erb H, Johnson JA, Murphy TH: Coordinate regulation of glutathione biosynthesis and release by Nrf2-expressing glia potently protects neurons from oxidative stress. J Neurosci 2003, 23:3394–3406
4. Shih AY, Imbeault S, Barakauskas V, Erb H, Jiang L, Li P, Murphy TH: Induction of the Nrf2-driven antioxidant response confers neuroprotection during mitochondrial stress in vivo. J Biol Chem 2005, 280:22925–22936
5. Vargas MR, Pehar M, Cassina P, Beckman JS, Barbeito L: Increased glutathione biosynthesis by Nrf2 activation in astrocytes prevents p75-dependent motor neuron apoptosis. J Neurochem 2006, 97:687–696
6. Shih AY, Li P, Murphy TH: A small-molecule-inducible Nrf2-mediated antioxidant response provides effective prophylaxis against cerebral ischemia in vivo. J Neurosci 2005, 25:10321–10335
7. McMahon M, Itoh K, Yamamoto M, Hayes JD: Keap1-dependent proteasomal degradation of transcription factor Nrf2 contributes to the negative regulation of antioxidant response element-driven gene expression. J Biol Chem 2003, 278:21592–21600
8. Nguyen T, Sherratt PJ, Nioi P, Yang CS, Pickett CB: Nrf2 controls constitutive and inducible expression of ARE-driven genes through a dynamic pathway involving nucleocytoplasmic shuttling by Keap1. J Biol Chem 2005, 280:32485–32492
9. Ma Q, Battelli L, Hubbs AF: Multiorgan autoimmune inflammation, enhanced lymphoproliferation, and impaired homeostasis of reactive oxygen species in mice lacking the antioxidant-activated transcription factor Nrf2. Am J Pathol 2006, 168:1960–1974
10. Benkovic SA, O'Callaghan JP, Miller DB: Sensitive indicators of injury reveal hippocampal damage in C57BL/6J mice treated with kainic acid in the absence of tonic-clonic seizures. Brain Res 2004, 1024:59–76
11. Schmued LC, Hopkins KJ: Fluoro-Jade B: a high affinity fluorescent marker for the localization of neuronal degeneration. Brain Res 2000, 874:123–130
12. Fernandes AM, Maurer-Morelli CV, Campos CB, Mello ML, Castilho RF, Langone F: Fluoro-Jade, but not Fluoro-Jade B, stains non-degenerating cells in brain and retina of embryonic and neonatal rats. Brain Res 2004, 1029:24–33
13. Eng LG, Ghirnikar RS, Lee YL: Glial fibrillary acidic protein: gFAP-thirty-one years (1969–2000). Neurochem Res 2000, 25:1439–1451
14. Norenberg MD: Astrocyte responses to CNS injury. J Neuropath Exp Neurol 1994, 53:213–220
15. O'Callaghan JP: Quantitative features of reactive gliosis following toxicant-induced damage of the CNS. Ann NY Acad Sci 1993, 679:195–210
16. O'Callaghan JP, Miller DB: Neurotoxicity profiles of substituted amphetamines in the C57BL/6J mouse. J Pharmacol Exp Ther 1994, 270:741–751
17. Little AR, O'Callaghan JP: The astrocyte response to neural injury: A review and reconsideration of key features. Edited by D Lester, W Slikker, P Lazarovici. London, Taylor and Francis Publishers, 2002, pp 233–265
18. Petzold A, Baker D, Pryce G, Keir G, Thompson EJ, Giovannoni G: Quantification of neurodegeneration by measurement of brain-specific proteins. J Neuroimmunol 2003, 138:45–48
19. Chan K, Lu R, Chang JC, Kan YW: NRF2, a member of the NFE2 family of transcription factors, is not essential for murine erythropoi-

esis, growth, and development. Proc Natl Acad Sci USA 1996, 93:13943–13948
20. Fix AS, Garman RH: Practical aspects of neuropathology: a technical guide for working with the nervous system. Toxicol Pathol 2000, 28:122–131
21. Karnovsky MJ: A formaldehyde-glutaraldehyde fixative of high osmolarity for use in electron microscopy. J Cell Biol 1965, 27:137A
22. Radovsky A, Mahler JF: Nervous system. Pathology of the Mouse. Edited by RR Maronpot, GA Boorman, BW Gaul. Vienna, IL, Cache River Press, 1999, pp 445–470
23. Hubbs AF, Battelli LA, Goldsmith WT, Porter DW, Frazer D, Friend S, Schwegler-Berry D, Mercer RR, Reynolds JS, Grote A, Castranova V, Kullman G, Fedan JS, Dowdy J, Jones WG: Necrosis of nasal and airway epithelium in rats inhaling vapors of artificial butter flavoring. Toxicol Appl Pharmacol 2002, 185:128–135
24. Eng LF, Ghirnikar RS: GFAP and astrogliosis. Brain Pathol 1994, 4:229–237
25. Raine CS: Oligodendrocytes and central nervous system myelin. Textbook of Neuropathology. Edited by RL Davis, DM Robertson. Baltimore, Williams and Wilkins, 1991, pp 115–141
26. Berger J, Moser HW, Forss-Petter S: Leukodystrophies: recent developments in genetics, molecular biology, pathogenesis and treatment. Curr Opin Neurol 2001, 14:305–312
27. Leegwater PA, Pronk JC, van der Knaap MS: Leukoencephalopathy with vanishing white matter: from magnetic resonance imaging pattern to five genes. J Child Neurol 2003, 18:639–645
28. Schiffmann R, van der Knaap MS: The latest on leukodystrophies. Curr Opin Neurol 2004, 17:187–192
29. Melov S, Schneider JA, Day BJ, Hinerfeld D, Coskun P, Mirra SS, Crapo JD, Wallace DC: A novel neurological phenotype in mice lacking mitochondrial manganese superoxide dismutase. Nat Genet 1998, 18:159–163
30. Melov S, Doctrow SR, Schneider JA, Haberson J, Patel M, Coskun PE, Huffman K, Wallace DC, Malfroy B: Lifespan extension and rescue of spongiform encephalopathy in superoxide dismutase 2 nullizygous mice treated with superoxide dismutase-catalase mimetics. J Neurosci 2001, 21:8348–8353
31. Carroll WM, Jennings AR, Mastaglia FL: Reactive glial cells in CNS demyelination contain both GC and GFAP. Brain Res 1987, 411:364–369
32. Cammer W, Tansey FA: Immunocytochemical staining of astrocytes, tanycytes, immature glial cells and ependymal cells in the central nervous system of the normal rat and the myelin-deficient mutant. Dev Neurosci 1989, 11:90–98
33. Fanarraga ML, Griffiths IR, McCulloch MC, Barrie JA, Kennedy PG, Brophy PJ: Rumpshaker: an X-linked mutation causing hypomyelination: developmental differences in myelination and glial cells between the optic nerve and spinal cord. Glia 1992, 5:161–170